

Study of the Synthesis and Bonding Properties of Reactive Hot-Melt Polyurethane Adhesive

Qiheng Tang, Jiyu He, Rongjie Yang, Qingsong Ai

School of Materials Science and Engineering, Beijing Institute of Technology, Haidian District, Beijing 100081, People's Republic of China

Correspondence to: J. He (E-mail: hejiyu@bit.edu.cn)

ABSTRACT: Reactive hot-melt polyurethane adhesive (RHMPA) is moisture-curing polyurethane (PU) adhesive whose main component is an isocyanate-terminated PU prepolymer that can be cured after application by reaction with ambient moisture. Two series of RHMPA containing poly(tetramethylene glycol) (PTMG) of different molecular weights and different degrees of polymerization of the hard segment have been successfully synthesized using a two-step bulk polymerization with 4,4'-diphenylmethane diisocyanate, PTMG, and 1,4-butanediol (1,4-BDO). The structure and basic properties of the RHMPA film have also been characterized by Fourier transform infrared spectroscopy (FTIR), thermogravimetric analysis, differential scanning calorimetry, dynamic mechanical analysis, atomic force microscopy, gel permeation chromatography (GPC), shore hardness (*A/D*), and tensile tests. The results show that the initial decomposition temperature is more than 250°C, and the tensile strength of the RHMPA film was greater than 15 MPa. The adhesive performance of the RHMPA with different hard-segment content was studied through studies of the single lap-shear strength and tensile strength of butt joints. The results show a general trend of the bonding strength increases with the hard-segment content at 25°C. The adhesive performance of RHMPA in different environments was also investigated. It was found that the RHMPA exhibited excellent bonding strength to thermoplastic polyurethane elastomer (TPU) when placed in the fridge at -20°C, hot water at 80°C, 1 M HCl solution (acid) at 25°C, and 1 M NaOH solution (alkaline) at 25°C for 10 h. © 2012 Wiley Periodicals, Inc. *J. Appl. Polym. Sci.* 000: 000–000, 2012

KEYWORDS: polyurethane; reactive hot melt adhesive; bulk polymerization; bonding strength; viscoelastic property

Received 9 April 2012; accepted 30 July 2012; published online

DOI: 10.1002/app.38415

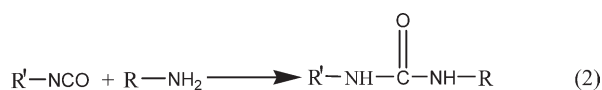
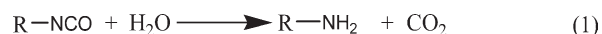
INTRODUCTION

Adhesives based on urea–formaldehyde and phenol–formaldehyde are very common,^{1–3} but are very sensitive to hydrolysis^{4,5} and stress scission.⁶ These adhesives also produce health hazards because of the formaldehyde they release.⁷ To overcome such problems, scientists are trying to develop new polymeric adhesives.^{8–10}

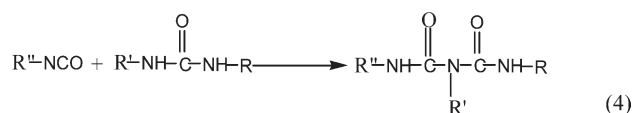
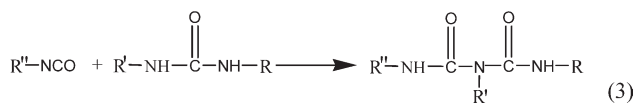
Over recent decades, so-called reactive hot-melt polyurethane adhesive (RHMPA) has attracted more and more attention both theoretically and for its applications because of its outstanding features compared to other kinds of adhesives, such as a high-initial adhesion strength, excellent adhesion to a multitude of substrates, good resistance to heat, chemicals, aging, easy processing, and environmental friendliness.^{11–13} RHMPA is 100% solid thermoplastic compound that contains neither solvent nor an aqueous carrier for the active adhesive components. The majority of RHMPA are composed of moisture-cured polyurethane (PU)/polyurea, a low-molecular weight, linear polymer with isocyanate (–NCO) end groups, which show good mechanical and weathering properties. The excellent bonding strength of the

RHMPA can be attributed to van der Waals forces, hydrogen bonding between the urethane and –OH from the substrate, and other factors. The RHMPA is applied in molten form, cooled to solidify, and subsequently cured by the reaction with ambient moisture.^{14–19}

After application, the RHMPA exhibit great strength as a result of crystallization of the urethane prepolymer. Water absorption from the atmosphere results in a subsequent cure reaction as follows, which increases the molecular weight:²⁰



A possible further reaction between urea, urethane, and a residual isocyanate group promotes crosslinking of the bulk adhesive.²⁰



A consequence of the cure reaction is that the urethane prepolymer, which is first linear, becomes crosslinked. As a result, the adhesion strength is greatly enhanced.

Although there are plenty of advantages in moisture curing of hot-melt adhesives, the moisture content of substrates must be high enough to accomplish complete crosslinking. Sometimes, the moisture is high enough in the environment, but the crystallization in the RHMPA also hinders moisture penetration into the system, thereby compromising adhesive performance. In addition, carbon dioxide bubbles can be formed, which also undermine the bonding strength of the adhesive.

In particular, when the adhesives are used in areas like food packaging, migration issues arise. Low-molecular weight monomeric diisocyanates may not react completely. Because their metabolites are migratory, they can then constitute a health hazard if they are capable of migration into the foodstuff. Monomeric isocyanates are harmful and unfortunately have a high-toxic potential. Even at low concentrations, they are capable of damaging the respiratory organs, eyes, and skin and may provoke allergic sensitization. If not applied properly, they can cause serious health problems.²¹

Stringent regulations have been prescribed by legislation,²¹ so that the concentration of residual amines must drop below the threshold limits specified for use in food packaging. Accordingly, it is essential to minimize migration as much as possible.

In some adhesive areas, a gap must be left between the substrates in order to adapt to the volume shrinkage of substrates at different temperatures and to the fluctuations in some difficult environments. In addition, the gel time of all of the adhesives available in the market is very short, which make them impossible to use over large areas.

To meet these strict demands and overcome the drawback of conventional RHMPA, operating a “green” production line is becoming a competitive advantage for companies in their relationships with customers., This work describes an investigation of several series of novel thermoplastic RHMPA consisting of 4,4'-diphenylmethane diisocyanate (MDI), poly(tetramethylene glycol) (PTMG), and 1,4-butanediol (1,4-BDO) as chain extenders. The RHMPA exhibits superior bonding strength to a thermoplastic polyurethane elastomer (TPU) and stainless steel and can therefore be widely used in various bonding situations. In addition, the tensile strength of the bulk RHMPA was very high, and so it can also be used for sealants.

EXPERIMENTAL

Materials

MDI was kindly provided by Beijing Co-Mens Company and used as received. PTMG ($M_n = 1000$ and 2000 g/mol) was purchased from Aladdin Reagent (China) Co. 1,4-BDO was purchased from Beijing Chemical Reagents Company. PTMG and 1,4-BDO were dried in a vacuum oven at 110°C for at least 2 h before use.

Preparation of RHMPA

The RHMPA was synthesized by two-step bulk polymerization with MDI, PTMG2000, and 1,4-BDO as chain extender. The synthesis was carried out in three-necked flask equipped with a mechanical stir. The right amount of PTMG was added to the flask with melt MDI at $60\text{--}70^\circ\text{C}$, and the reaction was controlled at 85°C and stirred for an hour, then the appropriate amount of 1,4-BDO was added to the melt, and the mixture was agitated vigorously until an homogeneous melt was obtained. All the synthesis process is under vacuum in order to prevent the generation of bubble. The hard-segment content was controlled at 20, 30, 40, and 50%, respectively. To synthesize the thermoplastic RHMPA, the molar ratio of NCO/OH is 1.00. The synthesis of PU is straightforward as shown in Scheme 1. The other kinds of RHMPA were prepared with the same procedure as described earlier, except that the PTMG1000 was added into the reactor instead of PTMG2000.

The sample designation codes provide information about the molecular weight of PTMG and the hard-segment content (i.e., RHMPA2000-20, indicating that RHMPA was synthesized using the PTMG with molecular weight of 2000 and the content of hard segment was 20%).

MEASUREMENTS

Fourier Transformed Infrared Spectroscopy

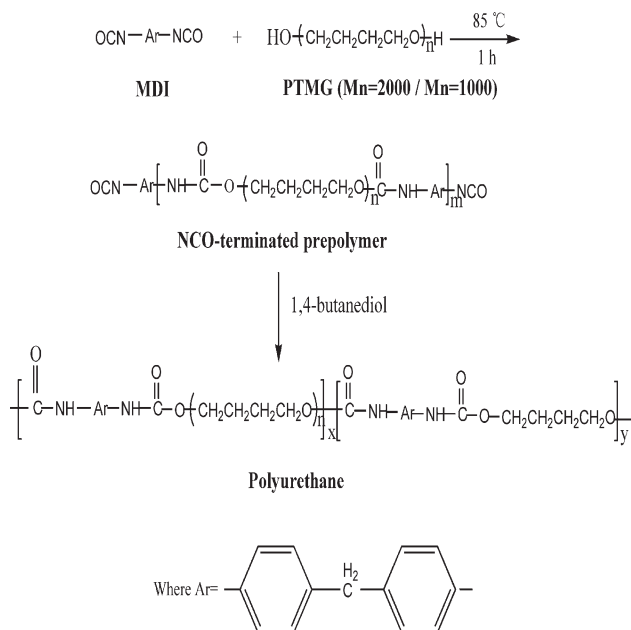
Fourier transform infrared spectroscopy (FTIR) analysis of the RHMPA was conducted by NICOLET 6700 IR spectrometer. The spectra were collected through 32 scans with a spectral resolution of 4 cm^{-1} .

Mechanical Properties

All the films of the adhesives were prepared by pouring the hot melt into a poly(tetrafluoroethylene) mold and were placed in an oven at 85°C for 25 h. The RHMPA films taken out from the ovens were cooled to the room temperature for at least 12 h. After that, the dumb-bell-shaped specimens were cut through using a metallic die. These specimens were stored at 23°C and 50% relative humidity for at least 12 h before testing. The specimens had a width of 3 mm in the neck and a thickness of 3.5 mm. The tensile tests were carried out with a cross-head deformation speed of 500 mm/min on a Universal Testing Machine Tension. The hardness of the RHMPA was measured using the Shore A/D method with a Zwick 7206/H04 hardness tester at 25°C .

Gel Time

The gel time was measured according to the method suggested by Degussa. Briefly, ~ 10 g of RHMPA at 85°C was applied to the wide side of a stainless steel plate whose dimension was 25 mm in length and 15 mm in width. A second block was



Scheme 1. The synthesis of polyurethane.

attached to the first one and carefully twisted. The gel time was defined as the time when the cubes could no longer be twisted.

Bonding Strength

Stainless steel plates and TPU elastomer sheets, $100 \times 15 \times 1 \text{ mm}^3$ and $100 \times 15 \times 1 \text{ mm}^3$, respectively, were used to perform single lap-shear tests. Two pieces of stainless steel or TPU sheet were placed together to form an overlap area measuring $25 \times 15 \text{ mm}^2$ and $15 \times 15 \text{ mm}^2$, respectively. The RHMPA described earlier was applied with a brush to both pieces of stainless steel or TPU sheet, and the two sheets were brought into contact and then put them into an oven at 85°C to cure. The bonding thickness or gap between the two sheets was maintained at 0.3 mm by means of 0.3-mm diameter wires. A sketch and dimensions of the butt joints of steel/steel and TPU/TPU are shown in Figure 1.

The stainless steel plates and TPU sheet were washed with tetrahydrofuran (THF) before adhesion. After cure, the samples were conditioned at room temperature (25°C) for 7 days before testing. The stretching rate used to determine the bonding strength of the stainless steel and TPU sheet was 5 and 500 mm/min, respectively. At least five samples were tested, and the average bonding strength was determined with at least 95% confidence level for statistical significance.

The effect of chain extension time on the adhesive properties was also investigated.

Chemical Resistance

TPU pieces bonded with the adhesives prepared from different polyols and with different hard-segment content were placed for 10 h in hot water at 80°C , 1 M HCl solution (acid) and 1 M NaOH (alkali) at room temperature, in the fridge at -20°C , respectively, and subjected to single lap-shear strength tests and measurement of the tensile strength of butt joints.

Steel pieces bonded with the adhesives prepared from different polyols and different hard-segment content were also subjected to similar tests at 50°C and -30°C in a high and low-temperature test chamber.

Gel Permeation Chromatography

The gel permeation chromatography (GPC) analysis was carried out on the Waters Breeze™ 2 HPLC System with a 2414 refractive index detector and a 1515 pump. The GPC columns were high temperature 3, 4, and 5, and the eluent used was THF. The RHMPA solutions were prepared by dissolving the samples in THF (4 mg/mL). The eluent was at a flow rate of 1 mL/min at 40°C .

Thermal Analysis

The thermal gravimetric analysis (TGA) was performed with a NETZSCH 209 F1 thermal analyzer at a heating rate of $10^\circ\text{C}/\text{min}$ under nitrogen atmosphere, and the temperature ranged from 40 to 550°C .

Differential scanning calorimetry (DSC) was performed by Netzsch 200 F3 instrument (Selb, Germany) in aluminum pans and scanned in the temperature range -60 to 240°C at a heating rate of $10^\circ\text{C}/\text{min}$ under nitrogen atmosphere.

Dynamic Mechanical Analysis

The viscoelastic behavior of the RHMPA ($5 \times 5 \times 3 \text{ mm}^3$) was analyzed by dynamic mechanical analysis (DMA) IV instrument (Rheometric Scientific, USA) in tensile mode at a frequency of 1 Hz and with a heating rate of $2^\circ\text{C}/\text{min}$ under nitrogen atmosphere, and the temperature range of study was from -90 to 50°C .

Atomic Force Microscopy

Atomic force microscopy (AFM) was carried out with a Multimode/NS-3 a microscope, in tapping mode in air at room temperature. To compare the structure of all investigated samples, the imaging scans were kept to $10 \mu\text{m}$. The samples were dissolved in THF and coated on a silicon substrate and then dried in vacuum at room temperature for 2 days.

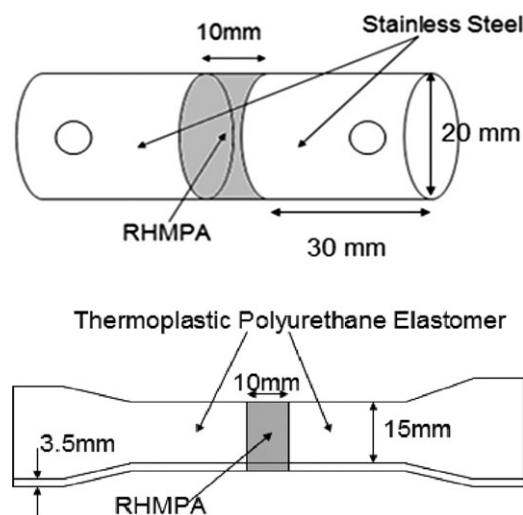


Figure 1. The models of tensile strength of butt joints for TPU/TPU and steel/steel.

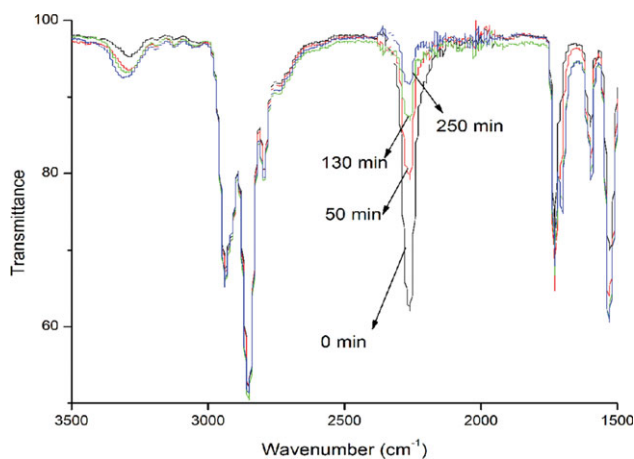


Figure 2. FTIR spectra of the RHMPA2000-20 at different chain extending time. [Color figure can be viewed in the online issue, which is available at wileyonlinelibrary.com.]

RESULTS AND DISCUSSION

Effect of Hard-Segment Content and Polyols on the Chain-Extending Rate Constants

The chain-extending reaction between NCO-terminated prepolymer and 1,4-BDO can be easily followed by recording FTIR spectra at various time intervals. For instance, the variations of FTIR spectra of RHMPA2000-20 with time at 85°C are shown in Figure 2. To relate conversion with absorbance changes of the area of isocyanate group, $-\text{NCO}$ stretching band appearing at around 2273 cm^{-1} , A_{NCO} , was measured at different times and normalized with the area of a reference peak; in this case, the C—H symmetric and antisymmetric stretching band spanning from 2950 to 2850 cm^{-1} approximately, A_{CH} , does not significantly change during reaction. Lambert–Beer law was assumed. Relative changes in molar absorptivity for the isocyanate and for the reference band during the reaction were considered to be equal.²² For this reason, the ratio between the absorbance of NCO and that of CH stretching vibration mode is taken as a measure of concentration of isocyanate groups for the purpose of evaluating kinetic parameters.

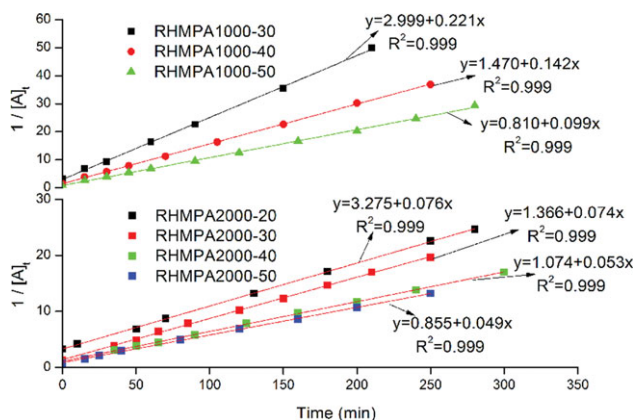


Figure 3. The second-order kinetic plots for RHMPA1000 system and RHMPA2000 system. [Color figure can be viewed in the online issue, which is available at wileyonlinelibrary.com.]

Table I. The Chain Extending Reaction Rate Constants from FTIR Spectroscopic Study

K (min ⁻¹)	RHMPA1000-20	RHMPA1000-30	RHMPA1000-40	RHMPA1000-50	RHMPA2000-20	RHMPA2000-30	RHMPA2000-40	RHMPA2000-50
Mole ratio	1 : 1 : 0	3.12 : 2.04 : 1.00	1.89 : 0.85 : 1.00	0.099	0.076	0.074	0.053	0.049
		1.52 : 0.47 : 1.00	1.62 : 0.31 : 1.00	2.36 : 1.36 : 1.00	1.62 : 0.56 : 1.00	1.32 : 0.31 : 1.00	1.20 : 0.20 : 1.00	
Mole ratio—the ratio of MDI:PTMG:1,4-BDO.								

Table II. Mechanical Properties of RHMPA

Sample designation	Tensile strength (MPa)	Elongation at break (%)	Gel time (min)	Hardness (shore A/D)
RHMPA1000-30	19.4 ± 1.5	537 ± 35	50	76
RHMPA1000-40	21.6 ± 1.3	500 ± 58	35	91
RHMPA1000-50	23.0 ± 0.8	435 ± 47	15	97
RHMPA2000-20	15.9 ± 2.5	679 ± 32	80	70
RHMPA2000-30	18.4 ± 1.5	609 ± 53	40	84
RHMPA2000-40	20.2 ± 0.5	583 ± 61	20	95
RHMPA2000-50	23.5 ± 1.0	375 ± 47	1.5	99

It has been established that the reaction between hydroxyl and isocyanate groups follows second-order kinetics.²³ When the ratio between the equivalents of NCO and OH groups is below unity, the kinetic expression can be written as follows:

$$1/[C_{\text{NCO}}]_t = kt + 1/[C_{\text{NCO}}]_0 \quad (5)$$

$[C_{\text{NCO}}]_0$ and $[C_{\text{NCO}}]_t$ are concentrations of NCO groups at the start of the reaction and at any given time t and k is second-order rate constant. When the absorbance is considered for concentration term, the kinetic equation may take the form as²⁴

$$1/[A]_t = kt + 1/[A]_0 \quad (6)$$

where

$$[A]_0 = \frac{A_{\text{NCO}, t=0}}{A_{\text{CH}, t=0}} \quad (7)$$

and

$$[A]_t = \frac{A_{\text{NCO}, t=t}}{A_{\text{CH}, t=t}} \quad (8)$$

Figure 3 displays the second-order plots for the reactions of the different prepolymers with 1,4-BDO from 0 to 300 min. In all cases, linear plots with good correlation coefficients were obtained, indicating that the reactions between the NCO-terminated prepolymer and 1,4-BDO curatives follow second-order kinetics, as reported by Reegen and Frisch.²³ The slopes of the straight line plots are the rate constants for the reactions. The second-order rate constants thus obtained for the different RHMPA systems are listed in Table I.

In Table I, it is apparent that the rate constant decreases with the increase of hard-segment content. With this increase, there will be more hydrogen bonds in the system, which will restrict the motions of molecular chains, reduce the intermolecular collision probability, and result in a decrease in the rate constants. It is also noted that the rate constants of RHMPA1000 are greater than those of RHMPA2000 for RHMPA samples with the same hard-segment content. This phenomenon can be ascribed to the activity of PTMG, that is, the lower is the molecular weight of PTMG, the higher is the activity. This higher activity makes a contribution to the rate constant.

According to the stoichiometric ratio, there is no 1,4-BDO in the RHMPA1000-20 system, and so there is no rate constant for the chain extending reaction, and this cannot be used as an RHMPA.

Mechanical Properties of RHMPA

The mechanical properties of RHMPA are summarized in Table II. In each series of RHMPA samples, an increase of the hard-segment content results in increased tensile strength and hardness as well as a decrease in the elongation at break. However, for RHMPA with the same hard-segment content, the tensile strength of the RHMPA1000 series is stronger than the corresponding member of the RHMPA2000 series. This is because the increase of hard-segment content produces increases in the hard-segment cohesion, hydrogen bonds, and phase-separated structure of the material, which account for the tensile strength. The hardness is therefore determined by the hard-segment content. The sample with high-mass fraction of hard-segment possesses more numerous physical crosslinking points and rigid groups and thus an increase in rigidity.

Table III. Single Lap Shear Strength of Steel/Steel After Various Chain Extending Time (MPa)

Sample designation	1 h	2.5 h	3.5 h	5 h	15 h	25 h
RHMPA1000-30	5.33	6.64	7.53	7.41	7.80	7.73
RHMPA1000-40	6.06	6.19	7.87	8.01	8.12	7.96
RHMPA1000-50	6.75	7.23	8.05	8.66	9.18	9.04
RHMPA2000-20	7.58	8.01	7.96	7.67	8.09	8.12
RHMPA2000-30	7.94	7.86	8.05	8.46	8.65	8.51
RHMPA2000-40	8.80	9.04	9.10	8.95	9.04	9.11

Table IV. Tensile Strength of Butt Joints of Steel/Steel After Various Chain Extending Time (MPa)

Sample designation	1 h	2.5 h	3.5 h	5 h	15 h	25 h
RHMPA1000-30	3.23c	4.47a	4.24a	4.23a	4.15a	4.23a
RHMPA1000-40	6.60c	8.16a	8.59a	8.78a	9.04a	8.91a
RHMPA1000-50	6.71a	7.40a	10.97a	12.47a	12.30	12.28a
RHMPA2000-20	2.91c	2.89c	3.11c	3.18c	3.46a	3.54a
RHMPA2000-30	5.14c	5.20c	5.28a	5.21a	5.64a	5.95a
RHMPA2000-40	5.95c	7.67c	7.95a	8.12a	9.25a	9.46a

c, cohesive failure of adhesive; a, adhesive failure of adhesive.

Table V. Tensile Strength of Butt Joints of TPU/TPU After Various Chain Extending Time (MPa)

Sample designation	1 h	2.5 h	3.5 h	5 h	15 h	25 h
RHMPA1000-30	4.39c	5.22c	5.04a	5.02a	4.82a	5.59a
RHMPA1000-40	5.20c	5.42c	5.91a	6.68a	6.57a	6.60a
RHMPA1000-50	8.69c	8.92a	9.25a	9.16a	9.20a	9.16a
RHMPA2000-20	4.82c	5.58c	6.32c	6.63a	6.79a	6.54a
RHMPA2000-30	5.12c	7.33c	7.53a	7.60a	7.60a	7.54a
RHMPA2000-40	6.60c	7.03c	7.14a	8.00a	8.09a	8.12a

c, cohesive failure of adhesive; a, adhesive failure of adhesive.

The gel times also decrease with the increase in hard-segment content, because the viscosity of the melting RHMPA increases. For RHMPA with equal hard-segment content, the gel time of the RHMPA2000 is lower than that of the RHMPA1000. This phenomenon might be related to the length of the molecular chain of the polyols. That is, the RHMPA2000 samples can crystallize more easily than those of the RHMPA1000 and, thus, decrease the gel time.

For RHMPA2000-50, the gel time is 1.5 min, and so it could not be used as RHMPA, because its gel time is too short for proper application.

Bonding Strength of RHMPA

The single lap-shear strength of TPU/TPU after various chain-extending times was also tested, but the adhesive performance was found to be so good that the TPU itself fractured, and so the results are not shown here. This is because there are many urethanes in the TPU, and then it can form lots of hydrogen bonding between the substrates. In addition, in essence, the RHMPA is also a kind of TPU, the solubility parameters of

RHMPA, and the TPU are very similar, and so the RHMPA can permeate into the TPU at the surface. The single lap-shear strength of steel/steel, the tensile strength of butt joints of steel/steel, and the tensile strength of butt joints of TPU/TPU after various chain extending times are shown in Tables III–V, respectively.

These data suggest that for all types of substrate, a general trend of the bonding strength increases with time. The bonding mechanism of the adhesive to the substrate can include van der Waals forces, hydrogen bonding, mechanical interlocking, and covalent bonding as well as cohesion energy.^{23,25,26} For the first few hours, the reaction is slow, as revealed by the low M_n of RHMPA in Table VI, and so the chemical bonding is not strong enough to hold joints. In this period, the bonding strength is predominantly attributed to mechanical interlocking, hydrogen bonds, and van der Waals forces between the adhesive and substrate (TPU and steel), and the mode of failure is cohesive failure of the adhesive. As the reaction continues, the M_n of RHMPA becomes higher, that is, the degree of reaction of the NCO-terminated

Table VI. M_n of RHMPA After Various Chain Extending Time

Sample designation	1 h	2.5 h	3.5 h	5 h	15 h	25 h
RHMPA1000-30	26,300	39,100	39,600	40,900	43,400	51,000
RHMPA1000-40	26,600	34,800	36,300	42,600	51,600	51,600
RHMPA1000-50	19,700	22,000	20,300	25,500	26,300	30,200
RHMPA2000-20	21,800	27,100	30,700	43,500	40,300	43,700
RHMPA2000-30	26,600	24,300	30,800	41,100	42,000	40,400
RHMPA2000-40	18,200	18,600	22,200	29,800	34,100	30,300

Table VII. Chemical Resistance of Tensile Strength of Butt Joints of TPU/TPU (MPa)

Sample designation	Original strength	-20°C	80°C hot water	1 mol/L HCl	1 mol/L NaOH
RHMPA1000-30	4.39	5.45	5.02	5.40	5.50
RHMPA1000-40	5.20	6.60	5.57	6.51	6.47
RHMPA1000-50	8.69	9.18	7.20	9.25	9.08
RHMPA2000-20	4.82	6.70	6.04	6.64	6.74
RHMPA2000-30	5.12	7.50	6.30	7.45	7.40
RHMPA2000-40	6.60	8.10	6.76	8.05	8.16

Table VIII. Bonding Strength of Steel/Steel at 50 and -60°C (MPa)

Sample designation	Original strength		-30°C		50°C	
	S	T	S	T	S	T
RHMPA1000-30	7.73	4.23	11.21	8.52	4.66	2.87
RHMPA1000-40	7.96	8.91	12.66	15.47	5.16	5.12
RHMPA1000-50	9.04	12.28	15.72	20.32	5.80	9.25
RHMPA2000-20	8.12	3.54	12.71	7.27	5.76	3.40
RHMPA2000-30	8.51	5.95	14.22	14.46	6.18	4.34
RHMPA2000-40	9.11	9.46	15.06	17.01	6.37	5.36

S, single lap-shear strength; T, tensile strength of butt joints.

prepolymer and 1,4-BDO is higher, which contributes to the cohesion energy. In this region, for the steel/steel and TPU/TPU substrates, the chemical bonding plays a dominant role in the adhesive performance, leading to an increase in the bonding strength with M_n . In this region, the adhesive forces include chemical bonding resulting from the reaction of the free $-NCO$ in the adhesive and the active hydrogen in the substrate, and more and more hydrogen bonding, as well as the cohesion energy of RHMPA, in addition to the force described earlier. However, it should also be noted that the increase is slow, because the interaction force between the

RHMPA and substrate (including TPU and steel) is almost complete, and the mechanism of failure is simple failure of the adhesive.

For the same RHMPA series and the same substrate, the higher the hard-segment content, the better the adhesion performance. This is because with an increase in the hard-segment content, the crystallization of RHMPA and the hydrogen-bonding effect between the RHMPA and substrate are stronger.²⁷ In addition, there are more free $-NCO$ that can react with the free $-OH$ in the substrate.

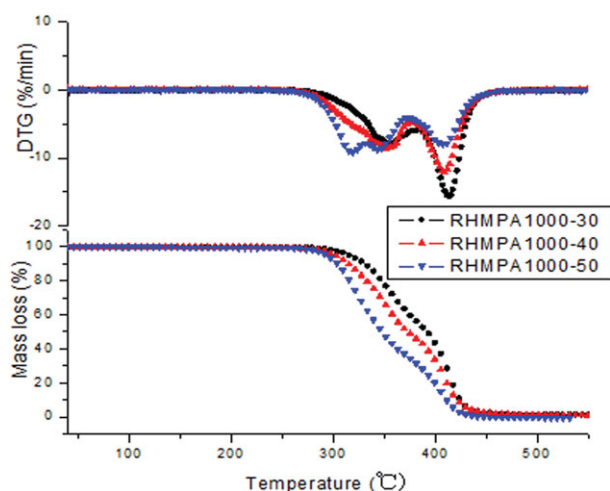


Figure 4. TGA and DTG curves of RHMPA1000 with different hard-segment content. [Color figure can be viewed in the online issue, which is available at wileyonlinelibrary.com.]

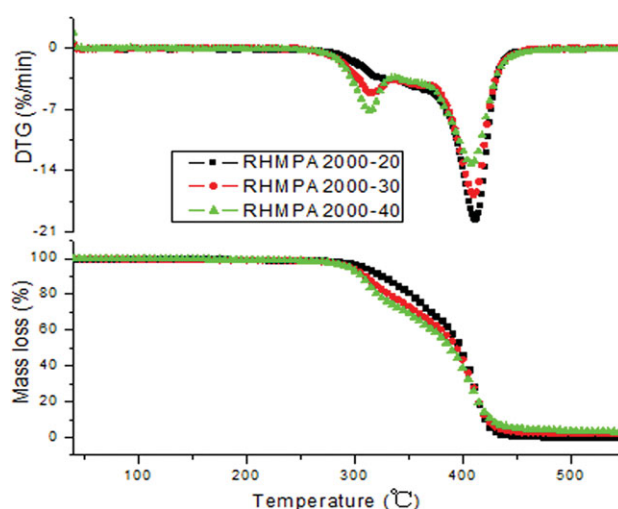


Figure 5. TGA and DTG curves of RHMPA2000 with different hard-segment content. [Color figure can be viewed in the online issue, which is available at wileyonlinelibrary.com.]

Table IX. Thermal Properties of RHMPA

Sample designation	T_5 (°C)	T_{10} (°C)	T_{\max} (°C)	ΔH_{mh} (J/g)	ΔH_{ms} (J/g)	ΔH_m (J/g)	T_g (°C)
RHMPA1000-30	312.0	327.9	413.7	0.6	4.8	5.5	-31.8
RHMPA1000-40	302.0	314.4	409.6	13.6	2.9	16.5	-28.9
RHMPA1000-50	294.1	304.7	409.3	21.8	0.6	21.8	-28.2
RHMPA2000-20	308.9	325.4	410.9	2.3	13.8	16.1	-51.9
RHMPA2000-30	295.6	309.9	410.0	6.1	7.7	19.7	-51.9
RHMPA2000-40	294.4	305.6	408.2	7.5	5.4	26.3	-53.2

T_5 , T_{10} defined as the temperatures of the samples with the weight loss of 5, 10, respectively.

T_{\max} defined as the decomposition temperatures of the soft segment.

ΔH_{mh} , ΔH_{ms} defined as the ΔH_m of hard-segment and soft-segment from the DSC curve, respectively.

Chemical and Temperature Influence on the Tensile Strength of Butt Joints of TPU/TPU

In Table VII, the results of the chemical resistance of the RHMPA used to make the TPU/TPU joints are presented. They show good resistance to cold water, acid, and alkaline solutions. However, the RHMPA adhesive performance was reduced to some extent in hot water. This could be due to rupture of some of the hydrogen bonding between the RHMPA and substrate.

High and Low-Temperature Resistance of the Bonding Strength of Steel/Steel

The bonding strength of the steel/steel joints was also investigated in a high and low-temperature test chamber at 50 and -60°C. The data are shown in Table VIII. At 50°C, the bonding strength decreases. The reason for this is the same as the effect of hot water on the RHMPA. However, at -60°C, the bonding strength increases significantly. At low temperature, the RHMPA exhibits higher cohesion energy and may generate more hydrogen bonding, which will contribute to the bonding strength.

Thermal Properties of RHMPA

TG Analysis of RHMPA. The thermal decomposition of RHMPA was investigated using TGA. The TGA curves and relevant data of RHMPA with different polyether diols and hard-segment content are shown in Figures 4 and 5, respectively. The thermal decomposition of RHMPA consisted of two steps, a result which is consistent with those of Xu et al.²⁸ and Kultys et al.²⁹ In the thermal decomposition, the first step began in the hard segments in the range 250–350°C and the second step in the soft segments beyond 400°C. It has been shown that RHMPA has high-thermal stability. In Table IX, T_5 and T_{10} decreased gradually as the hard-segment content increased, meaning that the thermal stability of the RHMPA also falls. However, for all PTMG, the T_{\max} remained almost unchanged, which shows that the thermal stability of RHMPA is not related to the molecular weight of PTMG.

At 500°C, the proportion of grayish char increases with the hard-segment content. This behavior suggests that higher hard-segment content may result in crosslinking structures, such as carbodiimide, during the process of thermal degradation.³⁰

For RHMPA with the same hard-segment content, the values of T_5 and T_{10} of RHMPA based on PTMG1000 are higher than those based on PTMG2000. Summarizing the results of the investigation of the thermal degradation for RHMPA based on

different molecular weight soft segments, it is found that the RHMPA based on PTMG 1000 are more thermally stable than those based on PTMG 2000.

DSC Analysis of RHMPA. Figure 6 shows the differential scanning calorimetry (DSC) thermogram for RHMPA1000 and RHMPA2000 with different hard-segment content. In Figure 6, the DSC curves of the RHMPA1000 series show one endothermic peak in the range 57.3–68.9°C and another endothermic peak in the range 134.6–157.9°C. These are associated with the melting point of the soft segment and hard segment, respectively. For the RHMPA2000, the endothermic peaks in the range 7.0–12.4°C and the endothermic peaks in the range 153–177.4°C can be assigned to the melting points of the soft segment and hard segment, respectively.

The increase of hard-segment content in the RHMPA slightly shifts the melting point of the hard segment to higher values, whereas the shift of the melting point of the soft segment is to lower values. There are more hydrogen bonds and better-ordered structures in the hard-segment region with the increase of hard-segment content, which was a contribution to the melting point. In contrast, there are fewer hydrogen bonds and less-ordered structures in the soft-segment region, which results in a lower melting point.

Crystalline units, if they exist, will make a significant contribution to the cohesive energy and thus to the adhesion strength.²⁷ Table IX shows that increasing the hard-segment content causes

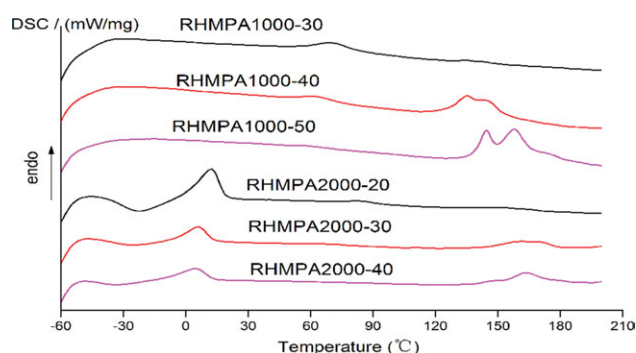


Figure 6. The DSC curves of RHMPA1000 and RHMPA2000 with different hard-segment content. [Color figure can be viewed in the online issue, which is available at wileyonlinelibrary.com.]

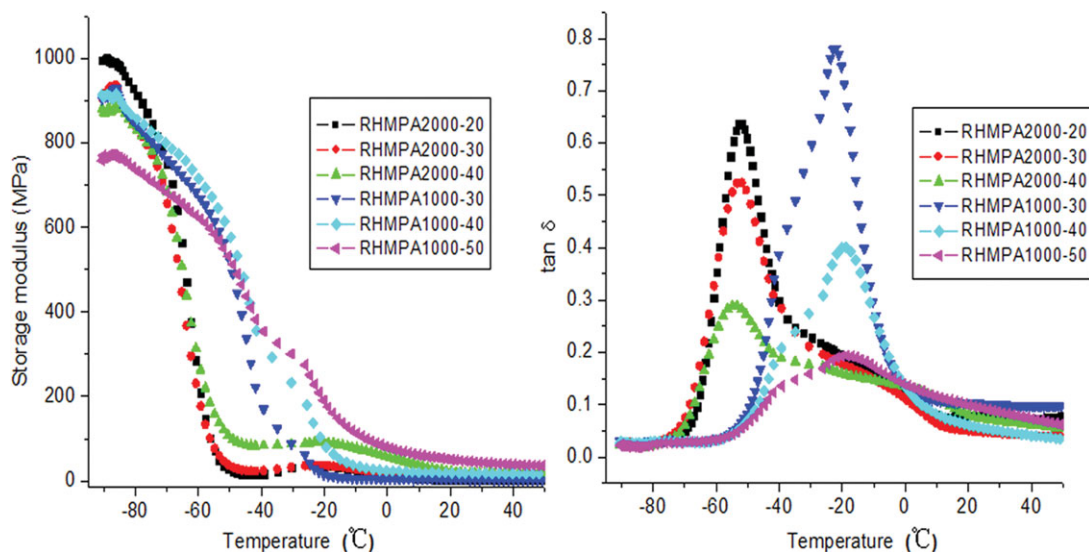


Figure 7. Storage modulus and $\tan \delta$ of RHMPA with different hard-segment content. [Color figure can be viewed in the online issue, which is available at wileyonlinelibrary.com.]

an increase in ΔH_m and consequently to the cohesion energy, which contributes to the bonding strength.

Dynamic Mechanical Analysis

The storage modulus (E') versus temperature curves for RHMPA films with different hard-segment content measured by dynamic mechanical analysis (DMA) are shown in Figure 7. The E' of the RHMPA decrease slowly upon heating from -95

to -60°C because of thermal expansion and then clearly decrease again from the initial temperature T_g due to the motion of chain segments. Moreover, for the same series of RHMPA, the thermomechanical stability increases with the hard-segment content, indicating that the material became less elastic due to the increase of hard-segment content. There is also a lot of hydrogen bonding and interaction forces, which will result in the cohesion energy increasing with hard-segment

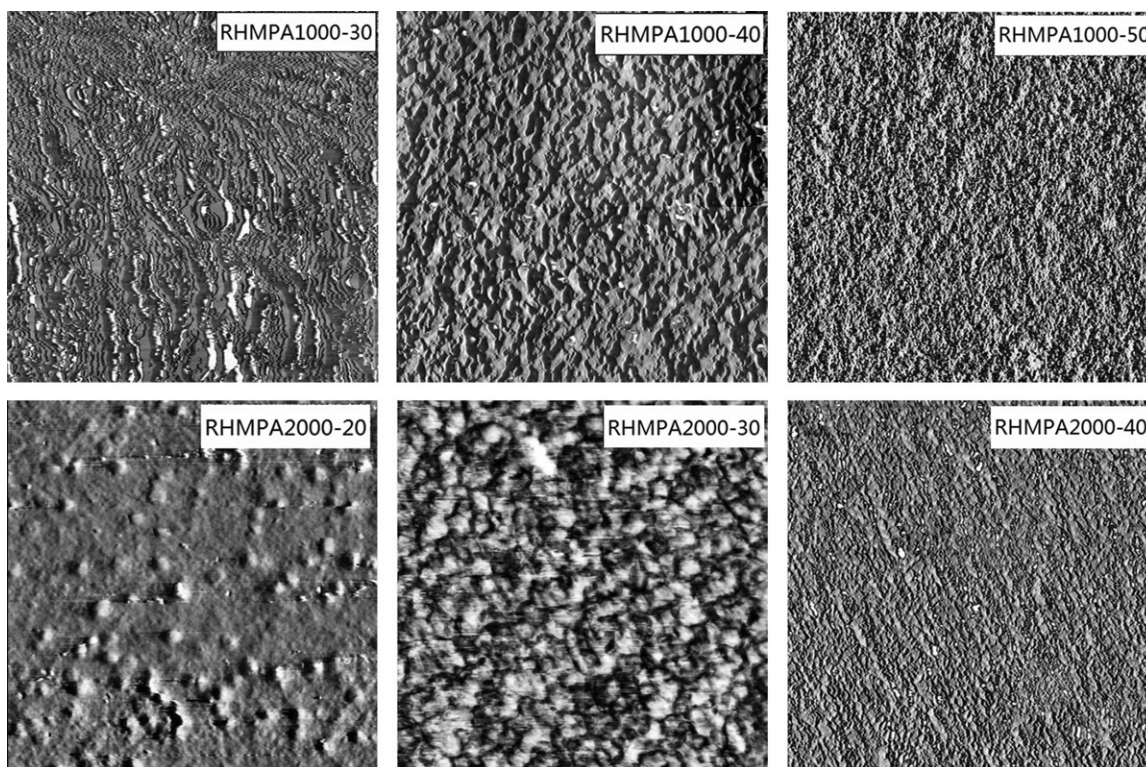


Figure 8. AFM phase images of RHMPA with different hard-segment content.

content. The bonding strength increases with E' , which is consistent with the analysis of the bonding strength section and corresponds well with the literature.^{31,32}

Although the storage modulus for both RHMPA2000 and RHMPA1000 decreased with temperature, it was noticed that the storage modulus for the RHMPA2000 samples decreased far more significantly than that of the RHMPA1000 from -60 to -20°C (ΔT). As $T_{g, \text{RHMPA2000}} < \Delta T < T_{g, \text{RHMPA1000}}$, the chain segment of RHMPA2000 could move easily and result in the significant E' decrease.

The curves for $\tan \delta$ of RHMPA2000 and RHMPA1000 are given in Figure 7, showing a slight decrease in $\tan \delta$ for the RHMPA2000 and RHMPA1000 series with the increase in the hard-segment content. This overall decrease is minimal, but indicates that the RHMPA2000 specimens lost some of their viscoelastic properties with increase in hard-segment content.

It is observed that the temperature of the glass transition, T_g , remains practically unchanged with the increase in hard-segment content in a given series. However, the T_g of RHMPA1000 is higher than that of RHMPA2000. This is because the length of PTMG1000 is shorter than that of PTMG2000, and so the molecular chains can become more compact, which results in strong interactions between molecular chains through hydrogen bonding.

Atomic Force Microscopy Analysis

To confirm the presence of the microphase separated morphology of the RHMPA with different hard-segment content, tapping-mode AFM experiments were performed. The phase images for a scanning range of $10 \mu\text{m}$ are shown in Figure 8. A typical two-phase structure can be observed. The comparatively bright part corresponds to the microphase of the aggregated hard segment of RHMPA, and the gray part corresponds to the microphase of the aggregated soft segment. It can be seen that the soft segment formed a continuous phase and the hard segment formed the dispersion phase. Moreover, with increasing hard-segment content, the extent of incompatibility of the two phases is greater, and the trend of microphase separation is more serious.

CONCLUSIONS

Two series of RHMPA, with different hard-segment content, were synthesized by classical two-step melt polymerization. For each series of RHMPA, the bonding strength, degree of crystallization, and storage modulus showed an increase with the hard-segment content. These results were characterized by single-lap strength, DSC, and DMA, respectively. For the different series of RHMPA with the same hard-segment content, the bonding strength of RHMPA2000 was greater than that of RHMPA1000. The RHMPA showed excellent thermal properties and good resistance to cold water, hot water, acid solutions, and alkaline solutions. The gel time of the RHMPA is very long, which means that the RHMPA can be used when the adhesive is needed to coat over large areas. In addition, the tensile strength of RHMPA film is very high, which means that it can be used as a sealant except for the adhesive.

REFERENCES

- White, J. T. *Adhes. Age*. **1981**, *24*, 19.
- Myres, G. E. *Adhes. Age*. **1988**, *31*, 31.
- Ebewele, R. O.; River, B. H.; Myres, G. E. *Adhes. Age*. **1993**, *49*, 229.
- Freeman, H. G.; Kreibich, R. E. *Forest. Prod. J.* **1968**, *18*, 39.
- Troughton, G. E.; Chow, S. J. *Inst. Wood Sci.* **1968**, *21*, 29.
- Dinwoodie, J. M.; Dinwoodie, J. M. *J. Inst. Wood Sci.* **1978**, *8*, 59.
- Wilson, J. B. *Adhes. Age*. **1981**, *24*, 41.
- John, N.; Joseph, R. J. *Appl. Polym. Sci.* **1998**, *68*, 1185.
- Osrekar, U.; Malavasic, T. *Int. J. Adhes. Adhes.* **1992**, *12*, 38.
- Desai, S. D.; Patel, J. V.; Sinha, V. K. *Int. J. Adhes. Adhes.* **2003**, *23*, 393.
- Hannes, F. *Mater. Tech.* **1990**, *78*, 93.
- Murray, B. D.; Autilio, R. D. TAPP Hot Melt Symposium. TAPP Press: Farmington, **1987**; p 95–99.
- Comyn, J. *Int. J. Adhes. Adhes.* **1998**, *18*, 247.
- Genova, R. D.; Harper, M. D.; Clay, W. A.; Cranley, P. E.; Hunte, M. K. *TAPPI J.* **1996**, *79*, 196.
- Waite, P. *Pigment Resin Technol.* **1997**, *26*, 300.
- Hung, J. M. Proceeding of the Hot Melt Symposium, Hilton Head Island, SC, June 10–13, **2001**; p 91–97.
- Oertel, G. *Polyurethane Handbook*, Vol. 30; Hanser: New York, **1986**; p 51–52.
- Kuo, P. L.; Liang, W. J.; Lin, C. L. *Macromol. Chem. Phys.* **2002**, *203*, 230.
- Li, X. R.; Fei, G. Q.; Wang, H. H. *J. Appl. Polym. Sci.* **2006**, *100*, 40.
- Cui, Y. J.; Hong, L.; Wang, X. L.; Tang, X. Z. *J. Appl. Polym. Sci.* **2003**, *89*, 2708.
- Michael, K. J. *Adhes. Interface.* **2006**, *7*, 53.
- Chaffanjon, P.; Grisby, R. A.; Rister, E. L.; Zimmerman, R. L. *J. Cell. Plast.* **2003**, *39*, 187.
- Reegen, S. L.; Frisch, K. C. In *Advances in Urethane Science and Technology*, Vol. 1; Frisch, K. C., Reegen, S. L., Eds.; Technomic Publishing: Westport, CT, **1971**.
- Manu, S. K.; Sekkar, V.; Scariah, K. J.; Varghese, T. L.; Mathew, S. J. *Appl. Polym. Sci.* **2008**, *110*, 908.
- Skeist, I. *Handbook of Adhesives*, 1st ed.; Van Nostrand Reinhold: New York, **1962**; Vol. 669.
- Packham, D. E. *Handbook of Adhesives*, 1st ed. London: Longman, **1992**; Vol. 407.
- Cui, Y. C.; Chen, D. H.; Wang, X. L.; Tang, X. Z. *Int. J. Adhes. Adhes.* **2002**, *22*, 317.
- Xu, Y.; Petrovic, Z.; Sas, S.; Wilkes, G. L. *Polymer* **2008**, *49*, 4248.
- Kultys, A.; Rogulska, M.; Gluchowska, H. *Polym. Int.* **2001**, *60*, 652.
- Bajsic, E. G.; Rek, V. *J. Appl. Polym. Sci.* **2001**, *79*, 864.
- Park, Y. J.; Kim, H. J. *J. Adhes. Sci. Technol.* **2003**, *17*, 1831.
- Park, Y. J.; Joo, H. S.; Kim, H. J.; Lee, Y. K. *Int. J. Adhes. Adhes.* **2006**, *26*, 571.